

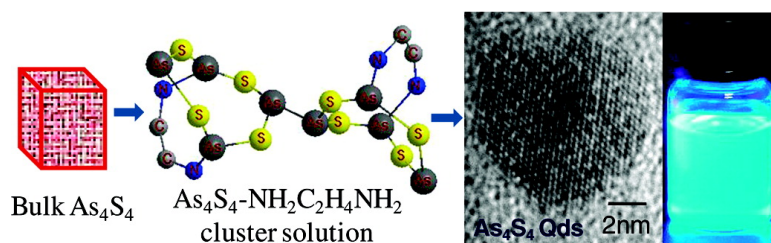
Communication

**Arsenic(II) Sulfide Quantum Dots Prepared by a Wet Process from its Bulk**

Junzhong Wang, Ming Lin, Tianyu Zhang, Yongli Yan, Paul C. Ho, Qing-Hua Xu, and Kian Ping Loh

*J. Am. Chem. Soc.*, **2008**, 130 (35), 11596-11597 • DOI: 10.1021/ja804436w • Publication Date (Web): 12 August 2008

Downloaded from <http://pubs.acs.org> on February 8, 2009



**More About This Article**

Additional resources and features associated with this article are available within the HTML version:

- Supporting Information
- Access to high resolution figures
- Links to articles and content related to this article
- Copyright permission to reproduce figures and/or text from this article

[View the Full Text HTML](#)

## Arsenic(II) Sulfide Quantum Dots Prepared by a Wet Process from its Bulk

Junzhong Wang,<sup>†</sup> Ming Lin,<sup>§</sup> Tianyu Zhang,<sup>‡</sup> Yongli Yan,<sup>†</sup> Paul C. Ho,<sup>‡</sup> Qing-Hua Xu,<sup>†</sup> and Kian Ping Loh<sup>\*†</sup>

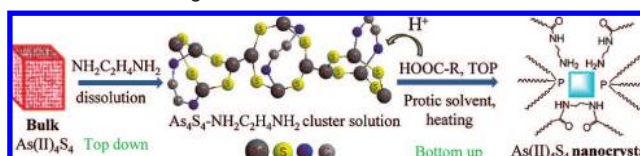
Departments of Chemistry and Pharmacy, National University of Singapore, 3 Science Drive 3, Singapore 117543 and Institute of Material Research and Engineering, 3 Research Link, Singapore 117602

Received June 11, 2008; E-mail: chmlhokp@nus.edu.sg

Quantum dots (QDs), in which the existence of carrier confinement allows only quantized states of the electron and holes, possess unique physical and optical properties that are useful for multiplexing and biosensing applications.<sup>1</sup> Much work has been carried out on the fabrication of II–VI, IV–VI, and III–V binary quantum dots.<sup>1–4</sup> However, to our knowledge, little work has been performed on the V–VI quantum dots. Semiconductors in the V–VI series have band gaps ranging from 2.2 eV for Sb<sub>2</sub>S<sub>3</sub> to 0.21 eV for Bi<sub>2</sub>Te<sub>3</sub>. These materials, especially those with narrower band gaps, demonstrate thermoelectric properties and are used in Peltier devices. There are no reported chemical routes applicable to the synthesis of arsenic sulfide QD thus far. The bulk form of arsenic sulfide can be found in natural minerals such as realgar ( $\alpha$ -As(II)<sub>4</sub>S<sub>4</sub>) and opigment (As(III)<sub>2</sub>S<sub>3</sub>) where the crystal structure, phase transformation, and stability of the various polymorphs have been investigated extensively.<sup>5</sup> Realgar was used as a drug by the Greeks and Chinese more than 2000 years ago.<sup>6a</sup> Recently realgar had also been investigated as a drug for curing promyelocytic leukemia.<sup>6</sup> In addition to therapeutic effects, amorphous arsenic sulfides are known to exhibit interesting optical properties such as photodarkening.<sup>7</sup> Here, we demonstrate that arsenic(II) sulfide nanocrystals could be prepared by bottom-up cluster-mediated synthesis from its bulk material. The nanocrystals can show size-dependent fluorescence ranging from 287 to 450 nm as well as two-photon upconversion.

One problem is the lack of soluble arsenic(II) precursors, but we are encouraged by the dissolution of its bulk material in ethylenediamine.<sup>8</sup> Early studies had shown that bulk arsenic(III) sulfide can be soluble in liquid ammonia<sup>8a</sup> or anhydrous amines.<sup>8b</sup> An arsenic(III) sulfide/ethylenediamine gelatinous system had been investigated in detail by Guiton and Pantano.<sup>8c</sup> We found that bulk arsenic(II) sulfide can be easily dissolved in ethylenediamine at room temperature to form a cluster solution (molecular complex, As<sub>4</sub>S<sub>4</sub>–NH<sub>2</sub>C<sub>2</sub>H<sub>4</sub>NH<sub>2</sub>). The nitrogen<sup>8c</sup> of ethylenediamine donate its lone pair to the empty *d*-orbitals of arsenic(II) as a Lewis base to form chelating bonds –As: NH<sub>2</sub>–CH<sub>2</sub>–CH<sub>2</sub>–H<sub>2</sub>N:As– between As and N, as shown in Scheme 1. <sup>1</sup>H NMR measurement (Figure S1a) shows a systematic downfield shift of the singlets of ethylenediamine with increasing concentration of As<sub>4</sub>S<sub>4</sub>, which indicates a higher degree of chelation to the bidentate ethylenediamine ligand. The cluster size is concentration dependent, as can be judged from changes in the absorption, photoluminescence (PL), and electrospray ionization mass spectra (Figure S1b,c). Both color and viscosity of the As<sub>4</sub>S<sub>4</sub>–NH<sub>2</sub>C<sub>2</sub>H<sub>4</sub>NH<sub>2</sub> solutions increase with increasing ratio of arsenic sulfide/ethylenediamine in the starting materials. Therefore As<sub>4</sub>S<sub>4</sub> exists as molecular complexes and chelates of the solvent, with gelation behavior<sup>8c</sup> due to the concentration effects of solvent extraction. It is possible that the size and chain number of As<sub>4</sub>S<sub>4</sub>–NH<sub>2</sub>C<sub>2</sub>H<sub>4</sub>NH<sub>2</sub> clusters are changing dynamically.

### Scheme 1. Preparation of Arsenic(II) Sulfide Nanocrystals from Its Bulk Material through Cluster-Mediate Transformation<sup>a</sup>



<sup>a</sup> Cluster structure of As<sub>4</sub>S<sub>4</sub>–NH<sub>2</sub>C<sub>2</sub>H<sub>4</sub>NH<sub>2</sub> is complex and dynamically varying, and only one possible unit is proposed here.

The synthesis of arsenic(II) sulfide nanocrystal is based on the transformation of the cluster solution of As<sub>4</sub>S<sub>4</sub>–NH<sub>2</sub>C<sub>2</sub>H<sub>4</sub>NH<sub>2</sub> to crystalline nanoparticles. The nanocrystal formation was controlled by the interplay of H-bonding and solvation in polar protic solvents and the consumption of ethylenediamine by reaction with carboxylic acid to form an amide as an in situ stabilizer (Scheme 1). The chelating bond between As and N is generally weak and can be readily destroyed by proton donor in polar protic solvents. The nucleation and growth of As<sub>4</sub>S<sub>4</sub> nanocrystal can occur in various protic solvents including ethanol, water, ethylene glycol, acetic acid, and acrylic acid. Thus the products can be dispersed to some extent in various solvents, which provide great flexibility for controlling the physical and chemical properties of the nanocrystals and its hybrids. Capping agents such as Trioctylphosphine (TOP) can improve the dispersion of nanocrystals in organic solvents. We discover that large amounts of nanocrystals with blue-cyan emission (gel method in experimental section in Supporting Information) can be prepared with the aid of acrylic acid to form a poly(acrylamide) hydrogel; this has the function of confining the size during growth as well as imparting the property of water solubility.

TEM images of the arsenic(II) sulfide nanocrystals are shown in Figure 1 and Figure S2 (Supporting Information), although the very low contrast of arsenic sulfide and easy adsorption of water by the amide stabilizer pose a challenge for high resolution imaging. Figure 1a shows nearly monodispersed nanocrystals with an ~3 nm particle size. Clear lattice fringes can be observed in larger

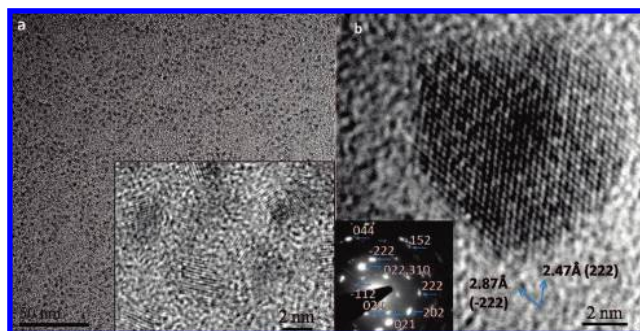


**Figure 1.** TEM images of arsenic(II) sulfide nanocrystals of (a) ~3 nm average size (inset HRTEM image (note: very low contrast); some particles are coupled) and (b) single particle of 9 nm (inset an ED pattern of close-packed nanocrystal assemblies).

<sup>†</sup> Department of Chemistry, National University of Singapore.

<sup>‡</sup> Department of Pharmacy, National University of Singapore.

<sup>§</sup> Institute of Material Research and Engineering.

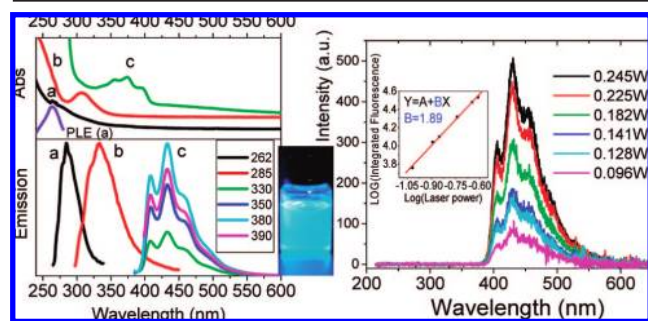


**Figure 2.** (Left) Size-dependent absorption (above) and normalized photoluminescence spectra (below) of solution samples (note: overlap of the absorption of nanocrystals and organic chemical groups at  $<350$  nm; the violet line inset is the photoluminescence excitation spectrum (PLE) of sample (a)). (a)  $\sim 3$  nm QD synthesized in ethanol, (b) 4–5 nm QD synthesized in 2-propanol, (c) 7–10 nm QD dispersed in THF (inset: fluorescence photograph under UV light). (Right) Upconverted emissions of sample (c) at room temperature excited by 790 nm pulse laser (inset: quadratic relationship between emission intensity and laser power of excitation).

particles of  $\sim 9$  nm in (b). The planes of  $(-222)$  and  $(222)$  with an interangle of  $58^\circ$  are displayed with  $d$ -spacings of 2.87 and 2.47 Å in Figure 1b, respectively. The inset ED pattern of 7–10 nm particles is in good agreement with XRD patterns (Figure S3a), which indicated that the product is monoclinic  $\beta$ -phase arsenic(II) sulfide (similar to the chemical source).<sup>5a,b</sup> Compositional analysis by energy-dispersive X-ray spectroscopy (EDX) reveals that the elemental ratio of arsenic/sulfide is close to 1.0. X-ray photoelectron spectroscopy (XPS) confirms the phase of arsenic(II) sulfide.<sup>5a,e</sup>

The arsenic(II) sulfide nanocrystals display clear features associated with size quantization effects such as a blue shift in absorption and near band edge emission.<sup>9</sup> Ultrasmall QDs of  $\sim 3$  nm size have an excitonic absorption centered at 262 nm (4.73 eV) with a near band gap emission peak centered at 287 nm (4.32 eV). QDs of 4–5 nm size have an excitonic absorption of  $\sim 310$  nm and also a near band gap emission peak of 340 nm. QDs of 7–10 nm size have several excitonic absorption peaks of 355, 373, and 395 nm (3.14 eV). The PL spectrum of sample 2(c) shows strong and sharp (average fwhm =  $\sim 25$  nm) emission peaks at 408 nm (3.04 eV) and 433 nm (2.86 eV), a shoulder at 455 nm, and a weak band at  $\sim 485$  nm, respectively (Figure 2c). Negligible shift in the emission wavelength was observed when the excitation wavelength was varied from 330 to 390 nm (Figure 2c), suggesting that the multiple peaks are not simply due to the effects of size heterogeneity. One explanation for the multiemission peaks for the 7–10 nm sized QDs is the presence of near-band-gap and defect-related shallow donor and acceptor or/and a deep-trap emission.<sup>10</sup> The blue emissions of  $\text{As}_4\text{S}_4$  nanocrystals are comparable to that of wide band gap ZnS (3.6 eV) or GaN (3.4 eV), which may be interesting for the fabrication of light-emitting diodes.<sup>1c</sup> Photoluminescence time decay (lifetime, 4.3 ns) exhibiting exponential decay kinetics was observed with pulse excitation at 400 nm for a solution sample in  $\text{HOC}_2\text{H}_4\text{OH}$  (Figure S4).

Upconversion fluorescence of the arsenic (II) sulfide nanocrystals in both hydrophilic and hydrophobic solvents was also observed. As shown in Figure 2 (right), the quadratic relationship between the excitation laser power and the fluorescence intensity, plus the necessity for pulsed laser excitation for luminescence detection, suggests that the upconversion fluorescence originates from a two-photon absorption process. Well-dispersed nanocrystals in THF (or  $\text{CHCl}_3$ ) can have a QY up to 50% (highly bright fluorescence in Figure 2(inset)). In water, the coating of the nanocrystal with a poly(acrylamide) shell prevents aggregation and affords a QY of 15%.

The in vitro cytotoxic effects of  $\text{As}_4\text{S}_4$  nanoparticles stabilized with ethylenediamine/acetic acid (EDAA) on selected human

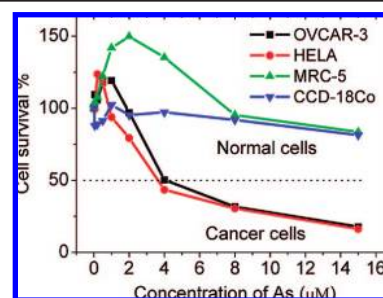


**Figure 3.** Dose–response curves of  $\text{As}_4\text{S}_4/\text{EDAA}$  nanoparticles treatment on the respective cancerous cell lines (OVCAR-3 and HeLa) and normal human fibroblast cells (MRC-5 and CCD-18Co) for 72 h.

ovarian (OVCAR-3) and cervical (HeLa) cancer cells were also investigated.  $\text{IC}_{50}$  (the concentration of a drug that is required for 50% inhibition in vitro) values are  $\sim 4 \mu\text{mol/L}$  of As for the two cancer cells, which is comparable to the reported mechanically prepared nanosized realgar.<sup>6c</sup> However,  $\text{As}_4\text{S}_4/\text{EDAA}$  shows a significantly smaller cytotoxicity on normal human lung fibroblast cells (MRC-5) and colonic fibroblast cells (CCD-18Co) (Figure 3) compared to nanosized realgar. Therefore  $\text{As}_4\text{S}_4$  nanoparticles exhibit good therapeutic efficacy.

In conclusion, a wet process of fabricating arsenic(II) sulfide nanocrystals from its bulk material through a cluster-mediated method has been demonstrated. The arsenic(II) sulfide nanocrystals show size-dependent emissions ranging from the UV to blue region as well as two-photon upconversion fluorescence. In view of its therapeutic effects and two photon fluorescence properties, arsenic sulfide nanocrystals can have potential applications in biomedicine and optoelectronics.

**Acknowledgment.** The work is supported by National University of Singapore Academic Grant R-143-000-265-112.

**Supporting Information Available:** Experimental procedures, additional TEM data, and phase characterization. This material is available free of charge via the Internet at <http://pubs.acs.org>.

## References

- (1) (a) Michalet, X.; Pinaud, F. F.; Bentolila, L. A.; Tsay, J. M.; Doose, S.; Li, J. J.; Sundaresan, G.; Wu, A. M.; Gambhir, S. S.; Weiss, S. *Science* **2005**, *307*, 538. (b) Bhattacharya, P.; Ghosh, S.; Stiff-Roberts, A. D. *Annu. Rev. Mater. Res.* **2004**, *34*, 1. (c) Taniyasu, Y.; Kasu, M.; Makimoto, T. *Nature* **2006**, *441*, 325.
- (2) Alivisatos, A. P. *Science* **1996**, *271*, 933. (a) Murray, C. B.; Kagan, C. R.; Bawendi, M. G. *Annu. Rev. Mater. Sci.* **2000**, *30*, 545.
- (3) Murray, C. B.; Noms, D. J.; Bawendi, M. G. *J. Am. Chem. Soc.* **1993**, *115*, 8706.
- (4) Leonard, D.; Krishnamurthy, M.; Reaves, C. M.; Denbaars, S. P.; Petroff, P. M. *Appl. Phys. Lett.* **1993**, *63*, 3203. (a) Green, M. *Curr. Opin. Solid State Mater. Sci.* **2002**, *6*, 355.
- (5) (a) Bonazzi, P.; S. Menchetti, S.; Pratesi, G.; Muniz-Miranda, M.; Sbrana, G. *Am. Mineral.* **1996**, *81*, 874. (b) Bonazzi, P.; Bindi, L.; Pratesi, G.; Menchetti, S. *Am. Mineral.* **2006**, *91*, 1323. (c) Špalt, Z.; Alberti, M.; Pená-Mández, E.; Havel, J. *Polyhedron* **2005**, *24*, 1417. (d) Douglass, D. L.; Shing, C.; Wang, G. E. *Am. Mineral.* **1992**, *77*, 1266. (e) Bullen, H. A.; Dorko, M. J.; Oman, J. K.; Garrett, S. J. *Surf. Sci.* **2003**, *531*, 319. (f) Rossetti, R.; Hull, R.; Gibson, J. M.; Brus, L. E. *J. Chem. Phys.* **1985**, *82*, 552. (g) Muniz-Miranda, M.; Sbrana, G.; Bonazzi, P.; Menchetti, S.; Pratesi, G. *Spectrochim. Acta, Part A* **1996**, *52*, 1391. (h) Roland, G. W. *Can. Mineral.* **1972**, *2*, 520.
- (6) (a) Zhu, J.; Chen, Z.; Lallemand-Breitenbach, V.; Thé, H. *Nat. Rev. Cancer* **2002**, *2*, 1. (b) Wang, L.; Zhou, G.; Liu, P.; Song, J.; Liang, Y.; Yan, X.; Xu, F.; Wang, B.; Mao, J.; Shen, Z.; Chen, S.; Chen, Z. *Proc. Natl. Acad. Sci. U.S.A.* **2008**, *105*, 4826. (c) Wu, J. Z.; Ho, P. C. *Eur. J. Pharm. Sci.* **2006**, *29*, 35.
- (7) Pfeiffer, G.; Paesler, M. A.; Agarwal, S. C. *J. Non-Cryst. Solids* **1991**, *130*, 111. (a) Uchino, T.; Clary, D. C.; Elliott, S. R. *Phys. Rev. Lett.* **2000**, *85*, 3305.
- (8) (a) Berzelius, J. J. *Ann. Chim. Phys.* **1826**, *32*, 166. (b) Chern, G. C.; Lauks, I. J. *Appl. Phys.* **1982**, *53*, 6979. (c) Guiton, T. A.; Pantano, C. G. *Chem. Mater.* **1989**, *1*, 558.
- (9) Babic, D.; Rabii, S.; Bernholc, J. *Phys. Rev. B* **1989**, *39*, 10831.
- (10) Yu, J. H.; Joo, J.; Park, H. M.; Baik, S. I.; Kim, Y. W.; Kim, S. C.; Hyeon, T. *J. Am. Chem. Soc.* **2005**, *127*, 5662. (a) Adarsh, K. V.; Sangunni, K. S.; Kokenyesi, S.; Ivan, I.; Shipljak, M. *J. Appl. Phys.* **2005**, *97*, 044314–1.

JA804436W